Available online at www.sciencedirect.com

ScienceDirect

Energy Procedia 8 (2011) 318–323

Energy Procedia

SiliconPV: 17-20 April 2011, Freiburg, Germany

# Analysis of local Al-doped back surface fields for high efficiency screen-printed solar cells

S. Gatz[a]*, K. Bothe[a], J. Müller[a], T. Dullweber[a], R. Brendel[a,b]

[a] *Institute for Solar Energy Hamelin (ISFH), Am Ohrberg 1, 31860 Emmerthal, Germany*
[b] *Institute for Solid-State Physics, Leibniz Universität Hannover, Appelstrasse 2, 30167 Hannover, Germany*

## Abstract

In this paper, we investigate the surface recombination of local screen-printed aluminum contacts applied to rear passivated solar cells. We measure the surface recombination velocity by microwave-detected photoconductance decay measurements on test wafers with various contact geometries and compare two different aluminum pastes. The aluminum paste which is optimized for local contacts shows a deep and uniform local back surface field that results in $S_{met}$ = 600 cm/s on 1.5 Ωcm *p*-type silicon. In contrast, a standard Al paste for full-area metallization shows a non-uniform back surface field and a $S_{met}$ of 2000 cm/s on the same material. We achieve an area-averaged rear surface recombination velocity $S_{rear}$ = (65 ± 20) cm/s for line contacts with a pitch of 2 mm. The application of the optimized paste to screen-printed solar cells with dielectric surface passivation results in efficiencies of up to 19.2 % with a $V_{oc}$ = 655 mV and a $J_{sc}$ = 38.4 mA/cm² on 125×125 mm² *p*-type Cz silicon wafers. The internal quantum efficiency analysis reveals $S_{rear}$ = (70 ± 30) cm/s which is in agreement with our lifetime results. Applying fine line screen-printing, efficiencies up to 19.4 % are demonstrated.



Keywords: Photovoltaics, Silicon, Solar Cells, Surface Passivation

## 1. Introduction

Industrial crystalline Si solar cells typically apply a full-area aluminum (Al) back surface field (BSF) at the rear. In this process, an Al paste is screen-printed and sintered at temperatures of 700-900°C in a belt furnace. The Al-BSF provides an ohmic contact and a moderate rear surface passivation with

* Corresponding author. Tel.: +49-5151-999-314; fax: +49-5151-999-400.
*E-mail address*: s.gatz@isfh.de

1876–6102 © 2011 Published by Elsevier Ltd. Selection and/or peer-review under responsibility of SiliconPV 2011.
Open access under CC BY-NC-ND license. doi:10.1016/j.egypro.2011.06.143

typical effective rear surface recombination velocities $S_{rear}$ ranging from 200 to 600 cm/s on 1-3 Ωcm *p*-type silicon [1,2]. In order to increase the cell efficiency, the passivation quality at the rear has to be improved. Various dielectric layers such as thermally grown silicon dioxide $SiO_2$ [3] or plasma-enhanced chemical vapor deposited (PECVD) $SiN_x$ [3], $SiC_x$ [4], $SiO_x$ [5] or $Al_2O_3$ deposited by atomic layer deposition [6], are promising candidates. A dielectric layer also improves the internal reflectivity which reduces absorption losses by the Al rear contact. For forming local metal contacts, the dielectric layer has to be locally removed before the Al screen printing e.g. by laser technique [7] or etching paste [8]. Certain process parameters seem to influence the local contact formation substantially. The dielectric opening size itself should therefore have a significant impact on the contact formation and the effective surface recombination below the contacts [7,8]. Previous structural investigations showed that by adding additives in a screen-printing Al paste one obtains a thicker and more homogenous local Al-BSF [9]. In this paper, we apply different Al screen-printing pastes to investigate their impact on the surface recombination velocity below the metalized contacts. Moreover we discuss these results by applying an appropriate contact structure on the rear side of screen-printed PERC solar cells.

## 2. Investigation of the surface recombination velocity

In order to characterize the surface recombination velocity of locally metalized rear surfaces, lifetime measurements are performed. We use 100×100 mm²-large, 210 µm-thick, 1.5 Ωcm, *p*-type, boron-doped, and shiny-etched Float-Zone silicon wafers. The wafers are cleaned in a wet chemical RCA process. The 100 nm-thick $SiN_x$ layer with refractive index $n = 2.05$ is deposited on both sides of the wafers by an in-line microwave PECVD system (SiNA, Roth & Rau). The deposition temperature is around 400 °C. On one side, the $SiN_x$ layer is locally ablated by a laser with pulse lengths of 10 picoseconds and a wavelength of 532 nm. As shown in Figure 1, we define 25×25 mm² areas with 120 µm-wide line openings, which differ in line pitch $p$ ranging from 300 µm to 3500 µm. The metallization is realized by full-area Al screen printing.

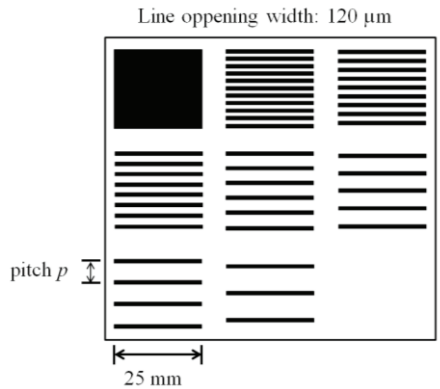


Fig. 1: Schematic sketch of the $SiN_x$ ablation pattern realized by picoseconds laser.

Besides the standard screen-printing Al paste, we use also an improved Al paste developed to form good contacts in local openings. After 5 minutes drying in a belt furnace (DO-HTO-5.200-210, Centrotherm) at 200 °C, the samples are fired in an additional belt furnace (DO-FF-8.600-300, Centrotherm) at typical set peak temperatures of 800 to 900 °C. An area with fully removed $SiN_x$ acts as BSF reference. Areas without $SiN_x$ ablation shows the impact of the Al paste on passivated areas. Spatially-resolved microwave-detected photoconductance decay (MWPCD) measurements provide mappings of the effective charge carrier lifetime $\tau_{eff}$. Applying the approach of Ref. 10 results in an area-averaged effective rear surface recombination velocity $S_{rear}$ for each single 25×25 mm² area. To determine

the local contact recombination velocity in the metalized areas $S_{met}$ we fit the captured data applying the equation developed by Fischer [10]

$$S_{rear} = \left( \frac{R_b - \rho W}{\rho D} + \frac{1}{f S_{met}} \right)^{-1} + \frac{S_{pass}}{1-f} \quad (1).$$

$S_{rear}$ is a function of the surface recombination velocities in metalized $S_{met}$ and passivated areas $S_{pass}$, and the metallization fraction $f$. The contribution of the base to the series resistance $R_b$ depends on the contact geometry [12]. Base resistivity $\rho$, thickness $W$ and diffusion coefficient $D$ of the wafers are known. Using a scanning electron microscope (SEM), we determine the contact line width $a$ after the firing step, and therefore the metallization fraction of the line contact pattern $f = a/p$ with contact pitch $p$. We observe an increase in line width between 40 and 70 µm when compared to the laser ablated line opening due to thermally activated dissolution of Si in the Al paste also at the contact edges below the dielectrics.

Figure 2 shows the effective rear surface recombination velocity $S_{rear}$ depending on the respective line pitch in each 25×25 mm² area. $S_{rear}$ decreases with increasing line pitch due to the decrease in metallization fraction. Applying the improved paste results in significantly lower $S_{rear}$ values compared to standard Al paste. By fitting experimental results using equation 1, we extract $S_{pass}$ = 20 cm/s, $S_{met}$ = 2000 cm/s for the standard Al paste and $S_{met}$ = 600 cm/s for the improved Al-paste. SEM images of contact cross sections are shown in Figure 2 b) and c). The improved Al-paste results in deep and homogeneous BSF formation over the entire contact opening. Even at the contact edges, the BSF is at least 7 µm-thick. In contrast, the BSF using the standard paste is formed only in the center of the contact. The edges of the openings show only a rudimentary or even no BSF at all. For both pastes, the $S_{rear}$ values of the full-area BSF lie around 500 cm/s which is the $S_{rear}$ value well known for conventional cells. Figure 2 shows that using a locally opened passivation layer reduces $S_{rear}$ by an order of magnitude compared to a full area Al-BSF: For 120 µm-wide line openings and a pitch of 2000 µm the screen-printed improved Al-paste results in $S_{rear}$ = (65 ± 20) cm/s compared to 400-600 cm/s for a full-area BSF. Similar samples passivated symmetrically by a stack of 10 to 20 nm-thick thermally grown $SiO_2$ and 200 nm-thick PECVD $SiN_x$ layer with refractive index $n$ = 2.05, are also investigated. Applying the improved paste for a line shaped contact pattern with line opening widths of 80 to 90 µm and pitch of 2000 µm, it results in $S_{rear}$ = (80 ± 20) cm/s.

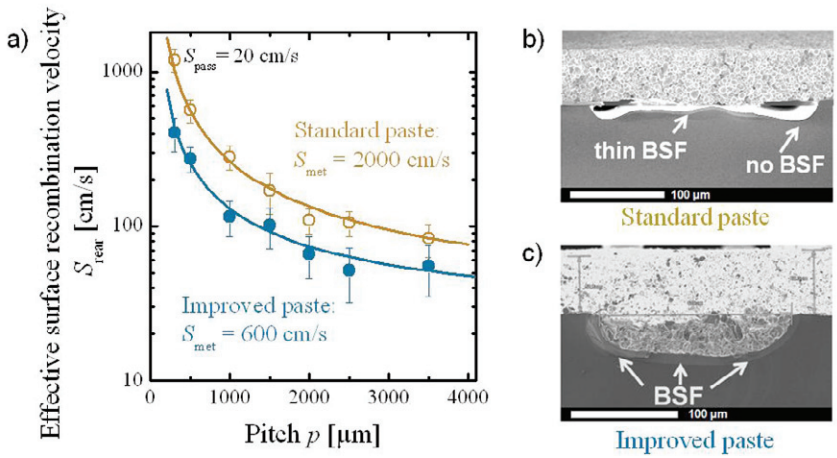


Fig. 2: a) Decrease of the rear surface recombination velocity $S_{rear}$ with increasing pitch due to a decrease in metallization. The symbols correspond to measurement results applying an $SiN_x$ passivation layer with standard Al paste (orange) and improved Al paste (blue), the lines correspond to the fits by using Equ.1. SEM images of contact cross sections b) and c) show deeper and more homogeneous Al-BSF in the local openings for the improved paste (c) compared to the contact formation with standard Al paste. The cross fractions are not perpendicular to the line direction.

## 3. High-efficient PERC solar cells with uniform emitter

We apply the improved screen-printing Al paste to the locally opened rear of a 125×125mm²-large, passivated emitter and rear solar cell (PERC) that we fabricate on 200 µm-thick, *p*-type 2 to 3 Ωcm boron-doped Cz-Si wafers. The schematic solar cell structure and a SEM image of the cross section are shown in Fig. 3. In the solar cell process a dielectric coating on the rear allows for a single side texturing and phosphorus diffusion using $POCl_3$. After simultaneously removing the protection layer at the rear and the phosphosilicate glass at the front by HF etch, a 15 minute dry thermal oxidation at 900°C results in 10 to 25 nm-thick thermally grown $SiO_2$ at both surfaces. As shown in Ref. [13], that short oxidation step varies the emitter profile slightly. The sheet resistance is (65±10) Ω/□ measured by a 4-point probe method. After removing the $SiO_2$ at the front, we deposit on both sides PECVD $SiN_x$ with refractive index $n$ = 2.05 at a deposition temperature of 400°C. Applying a thickness of 70 nm at the front we profit from its excellent anti reflection properties. The $SiN_x$ capping layer at the rear is 200 nm-thick. The $SiO_2/SiN_x$ rear side stack receives local line openings by the same laser system as described above. The opened line width is 80 to 90 µm, the pitch is 2000 µm. The screen-printed contacts to the emitter and to the base are formed by Ag and Al pastes, respectively. Each print process is completed by a 5 minute drying process in a belt furnace. The local Al-BSF (LBSF) forms during the co-firing step in the additional belt furnace with a set peak temperature of 860°C. Solar cells with a conventional full-area Al-BSF are also manufactured for reference purposes.

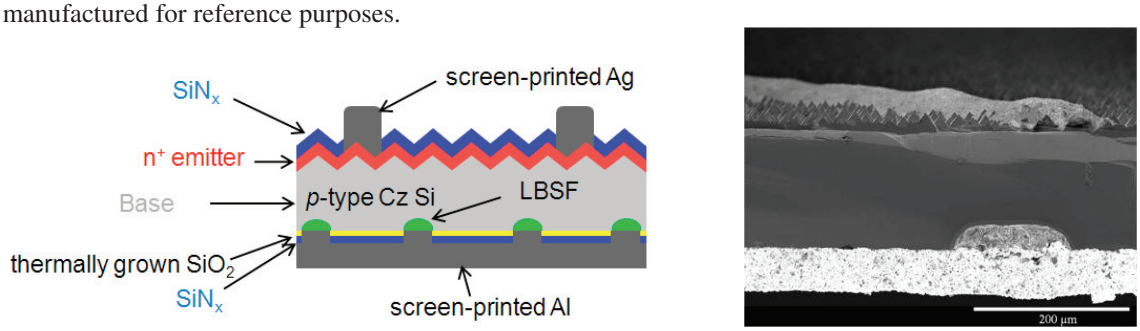


Fig. 3: Schematic (left) and SEM image (right) of a PERC solar cell with screen-printed front and rear contacts with $SiO_2$ / $SiN_x$ rear passivation. Note that the breaking edge in the SEM image is not perpendicular to the contact line direction at the front and the rear.

Table 1. Solar cell parameters measured under standard testing conditions (125 × 125 mm², pseudo-square, ~180 µm-thick, 2-3 Ωcm *p*-type boron-doped Cz-silicon)

| Cell-No | Rear configuration | Area [cm²] | Ag finger width | efficiency [%] | $V_{oc}$ [mV] | $J_{sc}$ [mA/cm²] | *FF* [%] |
|---|---|---|---|---|---|---|---|
| 1 | Local BSF $SiO_2$ / $SiN_x$ | 148.8 | 110 µm | 19.2 | 655 | 38.4 | 76.3 |
| 2 | Full-area Al-BSF | 146.6 | 110 µm | 18.0 | 629 | 36.6 | 78.1 |
| 3* | Local BSF $SiO_2$ / $SiN_x$ | 148.8 | 80 µm | 19.4 | 664 | 38.5 | 75.8 |

** PERC solar cell with fine-line Ag screen-printed front contacts, independently confirmed at Fraunhofer ISE CalLab [13].*

Table 1 shows the IV-data of both cell types which are processed as described above (Cell-No. 1 and 2). The open-circuit voltage $V_{oc}$ (655 mV) as well as the short-circuit current density $J_{sc}$ (38.4

mA/cm$^2$) of the PERC solar cell are significantly improved. This is also apparent from the IV-characteristics that are shown in Figure 4(a) as well. These improvements are due to a reduced rear surface recombination and the improved rear reflectance of the PERC cell. The improvement in absolute efficiency is + 1.2 %, resulting in a 19.2% efficient, fully screen-printed PERC device (cell No. 1 in table 1) when compared to a solar cell with full-area Al-BSF (cell No. 2 in table 1). For both cell structures, Figure 4(b) shows the measured internal quantum efficiencies (IQE) and reflectivity in the long-wavelength range. We observe a strong improvement in IQE and reflectivity due to the $SiO_2/SiN_x$ passivation stack. The value of $S_{rear}$ is extracted from these data by using the software LASSIE [14] which combines an extended IQE evaluation [15] and an improved optical model [16]. This results in $S_{rear} = (70 \pm 30)$ cm/s for the PERC structure compared to $S_{rear} = (500 \pm 100)$ cm/s for the full-area Al-BSF of a conventional screen-printed solar cell. The improved surface passivation at the rear combined with the slightly modified emitter profile result in an improvement of $V_{oc}$ from 629 mV to 655 mV. The decrease in surface recombination combined with an increase of the internal reflectivity at the rear improves $J_{sc}$ to 38.4 mA/cm² representing an increase of 1.8 mA/cm² compared to a full-area BSF reference cell. Applying "Print on Print" Ag screen printing technique [17] with apart from that quiet similar process flow [13], we profit from the reduced front finger width. It results in energy conversion efficiencies up to 19.4 % (cell No. 3 in table 1), $V_{oc} = 664$ mV and $J_{sc} = 38.5$ mA/cm$^2$.

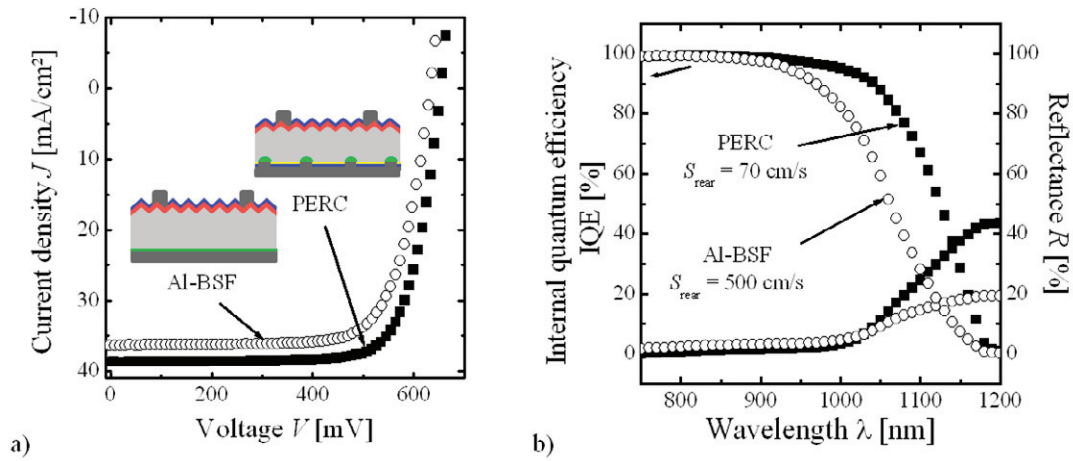


Fig. 4: Comparison between full-area Al-BSF (Cell-No. 2 in Tab. 1) and PERC solar cell (Cell-No. 1 in Tab. 1): (a) current-voltage measurements, (b) internal quantum efficiency and reflectivity measured immediately after the manufacturing process.

## 4. Conclusion

We have demonstrated measurements of the surface recombination of a PERC rear side. Thereby, the contact openings are realized by laser ablation prior to the screen-printing. The influence of the Al paste on the local Al-BSF formation is investigated. We achieved with a suitable Al paste surface recombination velocities below the contacts of 600 cm/s resulting in an effective surface recombination velocity at the rear of $S_{rear} = (65 \pm 20)$ cm/s with a line pitch of 2 mm. We demonstrate its application in industrially feasible large-area solar cells with passivated homogeneous emitter and rear achieving energy conversion efficiencies of up to 19.4 % on 125 × 125 mm² *p*-type 2 to 3 Ωcm boron-doped Czochralski silicon wafers. At the time of its first publication [13], the energy conversion efficiency of 19.4 % was the best value ever reported for fully screen-printed solar cells on large areas.

## Acknowledgements

We would like to thank A. Lohse for her help in processing the solar cells and T. Neubert for providing his assistance with sample preparation. Parts of this work are founded by the German Federal Ministry for the Environment, Nature Conservation and Nuclear Safety under Contract No. 0327529A. The contribution of DEK International is gratefully acknowledged.

## References

[1] S. Narasimha and A. Rohatgi, "Optimized Al back surface field techniques for Si solar cells" in: Proceedings 26th IEEE, PVSC, Anaheim, USA, 1997, p. 63

[2] S. Peters, "Rapid Thermal Processing of Crystalline Silicon Materials and Solar Cells", Ph.D. thesis, University Konstanz, 2004, p. 62

[3] A. W. Blakers, A. Wang, M. Adele, J. Zhao, and M. A. Green, "22.8% efficient silicon solar cell", Appl. Phys. Lett. **55**, 1989, p. 1363

[4] I. Martín, M. Vetter, A. Orpella, J. Puigdollers, A. Cuevas, and R. Alcubilla, "Surface passivation of p-type crystalline Si by plasma enhanced chemical vapor deposited amorphous $SiC_x$:H films", Appl. Phys. Lett. **79**, 2001, p. 2199

[5] M. Hoffmann, S. Kambor, C. Schmidt, D. Grambole, J. Rentsch, S. Glunz, and R. Preu, "Firing stable surface passivation using all-PECVD stacks of $SiO_x$:H and $SiN_x$:H", in: Proceedings 22nd EUPVSEC, Milano, Italy, 2007, p. 1030

[6] J. Schmidt, A. Merkle, R. Brendel, B. Hoex, M. C. M. van de Sanden, and W. M. M. Kessels, "Surface passivation of high-efficiency silicon solar cells by atomic-layer-deposited $Al_2O_3$", Prog. Photovolt. **16**(6), 2008, p. 461

[7] J. Müller, K. Bothe, S. Gatz, H. Plagwitz, G. Schubert, and R. Brendel, "Recombination at local Aluminum alloyed Silicon solar cell base contacts by dynamic infrared lifetime mapping", in: Proceedings 1st SiliconPV conference, Freiburg, 2011

[8] E. Urrejola, K. Peter, H. Plagwitz, and G. Schubert, "Silicon diffusion in aluminum for rear passivated solar cells", Applied Physics Letters 98, 2011, 153508

[9] V. Meemongkolkiat, K. Nakayashiki, D. S. Kim, S. Kim, A. Shaikh, A. Kuebelbeck, W. Stockum, and A. Rohatgi, "Investigation of modified screen-printing Al pastes for local back surface field formation, in: Proceedings 32th IEEE Photovoltaic Specialists Conference, Hawaii, USA, 2006, p. 1338

[10] J. Müller, K. Bothe, S. Gatz, F. Haase, C. Mader and R. Brendel , "Recombination at laser-processed local base contacts by dynamic infrared lifetime mapping", Journal of Applied Physics. 108, 2010, p. 124513

[11] B. Fischer, "Loss analysis of crystalline silicon solar cells using photoconductance and quantum efficiency measurements", PhD thesis at university Konstanz, Konstanz, 2003

[12] H. Plagwitz, M. Schaper, J. Schmidt, B. Terheiden, R. Brendel, "Analytical model for the optimization of locally contacted solar cells", in: Proceedings 31st IEEE Photovoltaic Specialists Conference, 2005, p. 999

[13] S. Gatz, H. Hannebauer, R. Hesse, F. Werner, A. Schmidt, T. Dullweber, J. Schmidt, K. Bothe, and R. Brendel, "19.4%-efficient large-area fully screen-printed silicon solar cells", Phys. Status Solidi RRL 5, No.4, p. 147

[14] www.pv-tools.de

[15] P. A. Basore, "Extended Spectral Analysis of Internal Quantum Efficiency"in: Proceedings 23rd IEEE PVSC, Louisville, USA, 1993, p.147

[16] R. Brendel, M. Hirsch, R. Plieninger, and J. H. Werner, "Quantum efficiency analysis of thin-layer silicon solar cells with back surface fields and optical confinement", IEEE Transaction on Electron Devices 43, 1996, p. 1104

[17] T. Falcon, "High Accuracy, High Aspect Ratio Metallization on Silicon Solar Cells Using a Print on Print Process", Proc. 25th EUPVSEC 2010, Valencia, Spain, p. 1651